

## DETERMINATION OF ELECTRICAL PARAMETERS AND THICKNESS OPTIMIZATION OF Cu<sub>2</sub>O/GaSb TANDEM SOLAR CELL USING SCAPS SOFTWARE

<sup>1</sup>Abdu Yunusa and <sup>2</sup>A. Yakubu

<sup>1</sup>Department of Physics, Bayero University, Kano, Nigeria.

<sup>2</sup> Kano State Secondary Schools Management Board, Kano, Nigeria.

### Abstract

*This paper presents a simulation work based on a four-terminal and mechanically stacked double junction tandem solar cell consisting of cuprous oxide (n- Cu<sub>2</sub>O /p- Cu<sub>2</sub>O) top p-n junction and Gallium Antimonide (n-GaSb/p-GaSb) bottom p-n junction. This is based on the appropriate band gaps of the materials which make them suitable for solar spectrum absorption. The work is aimed at enhancing the solar spectrum absorption of the n-GaSb/p-GaSb single junction solar cell and also improves on the efficiency of the Cu<sub>2</sub>O-based solar cells using simulation method. This was achieved using both materials in a tandem structure to form solar cell. This resulted in the absorption of the solar spectrum in the respective junctions of the proposed tandem cell using the junctions' cut-off wavelengths. The cell characterization was carried out using computer simulation software SCAPS and optimum performance of the cell was obtained. The work also determined the optimum thickness of the individual junctions corresponding to the highest efficiency of the sub- cells. The n- Cu<sub>2</sub>O /p- Cu<sub>2</sub>O top junction was simulated with 1000Wm<sup>-2</sup> incident power and obtained highest efficiency of 10.18% at an optimum thickness of 0.07µm. The n-GaSb/p-GaSb junction was simulated as a bottom junction of the tandem solar cell, and it received the solar flux of 622Wm<sup>-2</sup> in this structure. The n-GaSb/p-GaSb junction produced highest efficiency of 21.01% at an optimum thickness of 6.0µm. Therefore, the efficiency of the tandem solar cell n- Cu<sub>2</sub>O /p- Cu<sub>2</sub>O and n-GaSb/p-GaSb was found to be 31.2%. This result surpassed the theoretical value of the Shockley- Queisser efficiency limit for single junction solar cell of 30%. This was achieved by the combination of the two junctions in the tandem structure, in which the top junction absorbed the high energy photons of the solar flux and reduced the thermalisation effect in the bottom junction while the bottom junction which is the good absorber in the near infrared region absorbed with less thermalisation loss. This result is in agreement with the theoretical value predicted in literature using a combination of similar bandgaps.*

**Keywords:** photovoltaics, thickness optimization, tandem solar cells, Cu<sub>2</sub>O, GaSb, SCAPS, Cut-off wavelength

### 1. Introduction

The world energy demand has tremendously been increased due to increase in population and rapid development in technology. The conventional fossil fuel resources may not sustain current energy requirements beyond the next few decades and therefore, the need for inexpensive alternative energy resources [1]. There is also a growing concern over pollution, resource depletion, rising cost of producing electricity and possibility of climate change due to extensive usage of conventional fossil fuels and nuclear fuels [2,3]. These problems resulted in shifting focus towards renewable resources. Renewable energy from sources such as the sun, wind, rain and tides is safe and more reliable. The renewable energy resources are in abundance and by far the safest sources of energy available on earth [1].

The sun is outstanding amongst the potential new sources of energy because of its abundance, wide distribution and pollution free. The direct conversion of solar energy to electricity using photovoltaic (PV) cells is likely to be a good solution to the global energy problems; especially if practical economic means of direct conversion can be developed. The direct conversion of the solar energy to electricity is achieved using photovoltaic devices. The basic of such photovoltaic devices is the solar cell. Solar cells are solid state devices that

---

Correspondence Author: Abdu Y., Email: yunusa\_abdu@yahoo.com, Tel: +2348061192954

convert sunlight into electricity. The most common material for commercial solar cell construction is silicon (Si), others include Gallium Arsenide (GaAs), Cadmium Telluride (CdTe) and Copper Indium Gallium Selenide (CIGS) [4]. It was reported that more than 90% of the global PV markets rely on solar cells based on crystalline silicon (c-Si), with current efficiency record for single junction solar cells at 26.7% [5,6]. The efficiency of GaAs thin film solar cells was 27.6% [7] but later an improved value of about 29% was reported [6]. The efficiency of the CdTe single junction solar cell has been reported at 21%, while that of the CIGS solar cells is 23% [6] and all values were based on global AM1.5 unconcentrated sunlight. However, future development of the solar cells is predictably going to be lowered by high cost of material. Nevertheless, in the early 1961 Shockley and Queisser, in their work predicted theoretical efficiency limit of 30% for a single p-n junction solar cell illuminated by AM1.5 solar spectrum. The report also stated that photons with energy exceeding the band gap energy of the semiconductor lose the excess energy by thermalisation, which is the conversion of the excess energy to heat [8].

One of the most developed ways of enhancing the photon energy absorption of the solar cells, in order to surpass the Shockley-Queisser efficiency limit, is the use of multi-junction (MJ) structure [9,10]. This solar cell, typically, has two or more p-n junctions made of different materials having different band gap energy. The different junctions can be stacked on top of one another, with metallic contacts on the top and bottom materials of the solar cell. A stacked tandem device of this kind was first introduced in the late 1970s; and consisted of two subcells with each having a p-n junction: The bottom cell was based on gallium arsenide (GaAs) and the top cell (exposed to sunlight) was based on aluminium gallium arsenide. A different approach was later developed by the National Renewable Energy Laboratory (NREL) based on indium gallium phosphide (or InGaP alloy) junction on top of GaAs middle junction grown on a germanium (Ge) substrate. The InGaP, GaAs, and Ge of the triple-junction cell developed at NREL were selected because they have a desirable complement of bandgap energies and because they have a matching lattice constant [11]. Subsequent developments resulted in the replacement of the GaAs with InGaAs alloys. This stacked-subcells approach has resulted in MJ solar cells of conversion efficiency above 40% [12]. The idea is to absorb the various incident solar spectrums by the different junctions in order to improve the solar conversion efficiency of the entire tandem solar cell. This optimizes the light absorption and photocurrent generation of each junction of the sub-cells down to the narrow wavelength range [12].

This work proposes a two junctions four terminal tandem solar cell comprising of cuprous oxide (Cu<sub>2</sub>O) homojunction with the bandgap energy of 2.1eV as the top sub-cell. The semiconductor was intensively studied during 1970s and 1980s because it has the advantages of being low-cost, non-toxic, abundance of its raw material (which is copper) and simple production process [13,14]. While the other material forming the bottom sub-cell is Gallium Antimonide (GaSb) homojunction with band gap of 0.72eV and also non-toxic. This material is also good for electrical power conversion in the infrared spectral region, with the theoretical electrical power conversion efficiencies of 28% [15]. The combination of the two junctions is aimed at absorbing as much of the AM1.5 solar spectrum including the high energy photons and at the same time reducing the thermalization effect of the single junction of GaSb due to the solar illumination [8].

**2. Theoretical Background**

This work presents a four terminal tandem configuration. The structure requires a stack of Cu<sub>2</sub>O homojunction and GaSb homojunction as the top and bottom subcells respectively. The subcells are optically coupled by a non-absorbing layer.

Solar spectrum

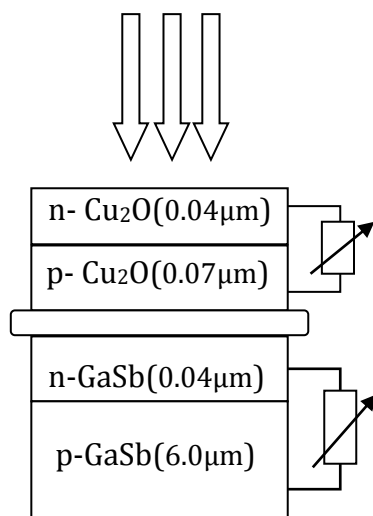


Figure 1. p-n Cu<sub>2</sub>O / p-n GaSb Four Terminal Tandem Solar Cell Structure.

The spectral distribution and short circuit current generation in the two junctions are expressed as [16];

$$J_{sc}^{(1)} = q \int_0^\infty \phi_{A.M1.5G}(\lambda)QE(\lambda)^{(1)}d\lambda \quad (1)$$

$$J_{sc}^{(2)} = q \int_0^\infty \phi_{A.M1.5G}(\lambda)T^{(1)}QE(\lambda)^{(2)}d\lambda \quad (2)$$

Where  $J_{sc}^{(1)}$  and  $J_{sc}^{(2)}$  are the short-circuit currents of top and bottom sub-cells,  $\phi_{A.M1.5G}(\lambda)$  is the incident photon flux,  $q$  is the electron charge,  $\phi_{A.M1.5G}(\lambda)T^{(1)}$  is the photon flux transmitted through the top junction,  $QE(\lambda)^{(1)}$  and  $QE(\lambda)^{(2)}$  are the quantum efficiencies of the two junctions respectively

The quantum efficiency (QE) measures the ratio of the amount of electron-hole pairs created to the incident photons at a given wavelength  $\lambda$  and is given by

$$QE_i(\lambda) = \frac{J_{sci}(\lambda)}{\phi_i(\lambda)} \quad (3)$$

where  $\phi_i(\lambda)$  is the photon flux of the corresponding incident light on subcell  $i$  and  $QE_i(\lambda)$  is the quantum efficiency of the subcell  $i$ .

The value of QE ( $\lambda$ ) is obtained by linking it with the absorption coefficient  $\alpha$  ( $\lambda$ ). Assuming each photon absorbed by a cell creates an electron/hole pair;

$$QE(\lambda)^{(i)} = 1 - \exp(-\alpha W) \quad (4)$$

where the superscript ( $i$ ) refers to the top cell and  $W$  is the cells thickness and  $\exp(-\alpha W)$  is the percentage of incident light which is not absorbed by the sub cell  $i$  (transmitted light). From equation (4), the light transmitted through the top cell and incident on the bottom cell is given by

$$= T^{(i)} = 1 - QE(\lambda)^{(i)} \quad (5)$$

Assuming only Photons with energy below the band gap of the  $Cu_2O$  top junction cell are transmitted to the GaSb bottom cell where a large fraction is absorbed. To make this possible, the top cell is also assumed to be infinitely thick. In this case, in equation (5) the transmission of the above band gap photons through the top junction,

$$T^{(i)} = \exp(-\alpha W) = 0 \text{ so that } QE(\lambda)^{(i)} = 1 \quad (6)$$

For all photon energies above  $Cu_2O$  top p-n junction's band gap energy,  $E_{gt}$ , also  $T^{(i)}(\lambda) = 1$  otherwise. So that Equations (1) and (2) can be approximated as;

$$J_{sc}^{(1)} = q \int_0^{\lambda_t} \phi_{A.M1.5G}(\lambda)d\lambda \quad (7)$$

$$J_{sc}^{(2)} = q \int_{\lambda_t}^{\lambda_b} \phi_{A.M1.5G}(\lambda)d\lambda \quad (8)$$

where  $\lambda_b = hc/E_{gb}$  and  $\lambda_t = hc/E_{gt}$  are called critical, or cutoff wavelengths which correspond to the band gaps of the top and bottom cells respectively. If the wavelength of the radiation exceeds this value, then the energy of the photon is less than the semiconductor bandgap energy ( $E_g$ ) and such a photon cannot cause a valence band electron to enter the conduction band [17], Singh & Ravindra formulated this wavelength as [18];

$$\lambda_g = \frac{1240}{E_g(eV)}(nm) \quad (9)$$

The value of cutoff wavelength for the  $Cu_2O$  top p-n junction with band gap 2.1eV,  $\lambda_t=590nm$  and similarly for the GaSb bottom p-n junction of 0.72eV band gap,  $\lambda_b=1722nm$  (calculated). Substituting the cutoff wavelength values in equations (7) and (8), they become;

$$J_{sc}^{(1)} = q \int_0^{590nm} \phi_{A.M1.5G}(\lambda)d\lambda \quad (10)$$

$$J_{sc}^{(2)} = q \int_{590nm}^{1722nm} \phi_{A.M1.5G}(\lambda)d\lambda \quad (11)$$

This implies that, using solar spectrum of A.M1.5 to illuminate this structure, the  $Cu_2O$  p-n junction absorption is assumed to be in the ultraviolet and part of visible range of solar spectrum while the GaSb p-n junction takes over from there to 1722nm in the near infrared region.

Absorption coefficient  $\alpha$  ( $\lambda$ ) is the number of photons absorbed per unit length of the material which is given by the analytical approximation;

$$\alpha(\lambda) = \alpha_o \left( \frac{E_\phi(\lambda) - E_g}{kT} \right)^{1/2} \quad (12)$$

where  $\alpha_o$  is the characteristic absorption coefficient for the material,  $E_\phi(\lambda) = hc/\lambda$  is the incident photon energy at wavelength  $\lambda$ ,  $E_g$  is band gap energy of a semiconductor,  $k$  is the Boltzmann constant, and  $T$  is the cell temperature.

The efficiency of the four terminal tandem cell whose junctions are optically coupled and electrically independent, is determined by the sum of the efficiencies of the junctions [19,20,21].

$$\eta_{Cu2O/GaSb \text{ tandem}} = \eta_{Cu2O} + \eta_{GaSb} \quad (13)$$

### 3. Simulation Method

This section presents the simulation procedure of Cu<sub>2</sub>O-GaSb four-terminal tandem solar cell which was conducted using SCAPS version 3.3.0.6. The simulation was carried out under standard test condition of solar incident power corresponding to air mass AM1.5 (1000W/m<sup>2</sup>), and ambient temperature of 300K. The parameters of the Cu<sub>2</sub>O and GaSb used in the problem definition panel of the SCAPS software are contained in table 1 [14,15,22,23].

Table 1. Properties of Cu<sub>2</sub>O and GaSb materials used in SCAPS simulation software

Parameter	Cu <sub>2</sub> O	GaSb
Band Gap (eV)	2.10	0.72
Dielectric constant at 300K	7.9	15.7
Electron mobility $\mu_n$ at 300K (cm <sup>2</sup> /Vs)	200	5650
Hole mobility $\mu_h$ at 300K (cm <sup>2</sup> /Vs)	100	875
Density of electrons in the conduction band, $N_c$ (cm <sup>-3</sup> )	$2.43 \times 10^{19}$	$2.078 \times 10^{17}$
Density of holes in the valence band, $N_v$ (cm <sup>-3</sup> )	$1.34 \times 10^{19}$	$1.770 \times 10^{19}$
Acceptor or donor density, $N_A$ or $N_D$ (cm <sup>-3</sup> )	$N_A = 1 \times 10^{17}$ $N_D = 2 \times 10^{18}$ (fitted)	$N_A = 5 \times 10^{19}$ $N_D = 2 \times 10^{18}$
Capture cross section of electrons ( $\sigma_e$ )(cm <sup>2</sup> )	$1.00 \times 10^{-8}$	$8 \times 10^{-19}$
capture cross section of holes ( $\sigma_p$ )(cm <sup>2</sup> )	$1.00 \times 10^{-11}$	$9 \times 10^{-15}$
electron effective mass, $m^*_e(m_0)$	0.14	0.047
hole effective mass, $m^*_p(m_0)$	0.66	0.5
Electron affinity $\chi_e$ (eV)	3.2	4.5
Electron thermal velocity ( $v_{th}$ , cm/s)	$10^7$	$5 \times 10^7$
Hole thermal velocity ( $v_{th}$ , cm/s)	$10^7$	$2 \times 10^7$
Absorption constant (m <sup>-1</sup> )	$5 \times 10^5$	$10^5$

#### Simulation of the proposed Cu<sub>2</sub>O/GaSb four-terminal tandem cell

To simulate the four-terminal Cu<sub>2</sub>O/GaSb tandem cell, the top and bottom junctions were simulated separately. This was done in order to examine the spectrum bands absorbed by the respective junctions of the tandem cell. The performances of these junctions were then added up to give the total response of the tandem cell in accordance with equation (13). The values of the cutoff wavelengths for the top and bottom junctions were used in the SCAPS action panel's spectrum cutoff settings during the simulation of the GaSb bottom junction. This was done so as to filter out the photons which are within the absorption range of the top Cu<sub>2</sub>O p-n junction from reaching the bottom GaSb p-n junction. In this work, the n-GaSb/p-GaSb bottom cell receives the filtered photon flux of 622W/m<sup>2</sup> (calculated by SCAPS), as described by equation (12). The simulation flow chart for both top and bottom junction is the same and is shown in Figure, 2. The only difference is in the third step after 'Run SCAPS' where the cutoff wavelength corresponding to 622W/m<sup>2</sup> incident power was selected in the case of the bottom junction.

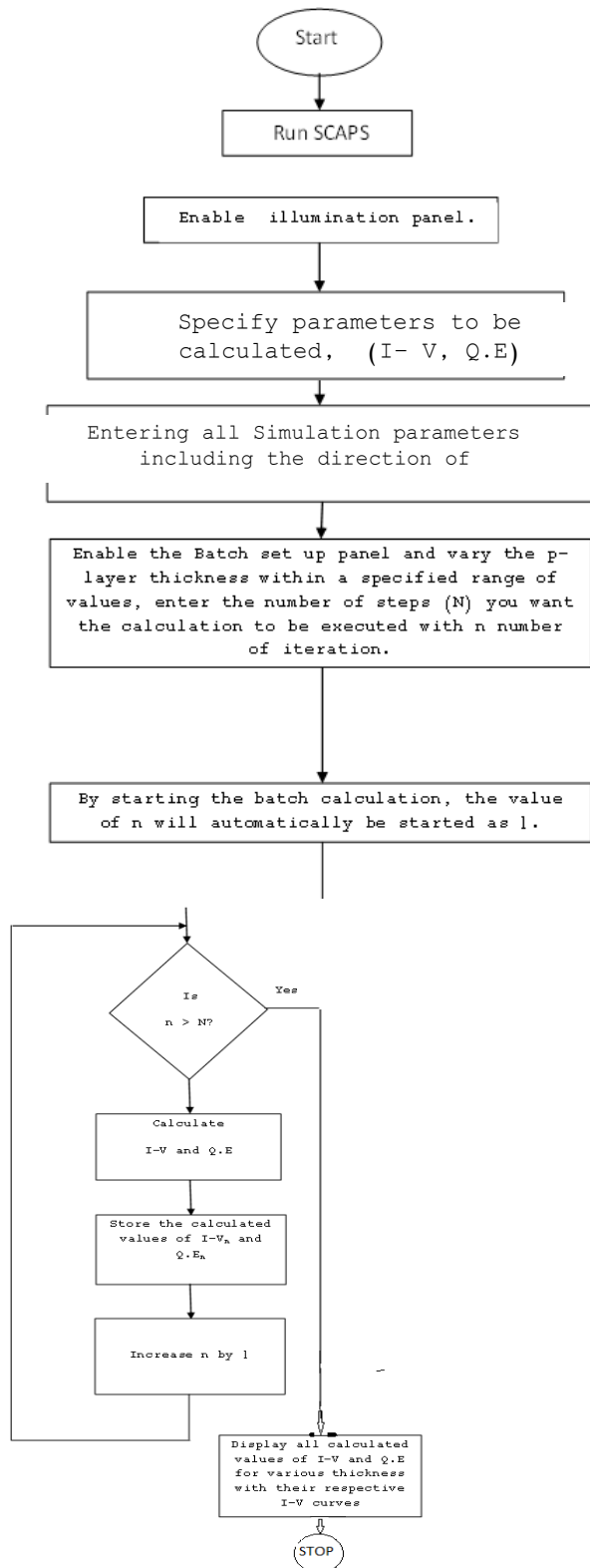


Figure 2: Simulation Flow Chart of the Top and Bottom single Junctions

Firstly, using the incident solar photon flux of  $1000\text{W/m}^2$ , the top single junction of n-  $\text{Cu}_2\text{O}$  /p- $\text{Cu}_2\text{O}$  was simulated. The operation of the junction under various thicknesses was evaluated. The efficiency of this single junction as a function of thickness was subsequently determined.

Secondly, the simulation study of the n-GaSb/ p-GaSb was carried out using two separate solar flux values. This was as a result of the n-GaSb/ p-GaSb being used in this case as a bottom junction. The amount of the incident flux reaching the bottom junction was calculated to be  $622\text{W/m}^2$ . Therefore, the single junction of n-GaSb/ p-GaSb was simulated using  $1000\text{W/m}^2$  and  $622\text{W/m}^2$  respectively, and the efficiency as a function of thickness for both cases also determined for the sub-cell.

Finally, the efficiency of the four-terminal tandem solar cell was determined. This was done by summing up the efficiencies of the top and the bottom sub-cells using equation (13).

#### 4. Results and Discussion

The simulation results of the single n- $\text{Cu}_2\text{O}$ /p- $\text{Cu}_2\text{O}$  top junction and that of the single n-GaSb/p-GaSb bottom junction are presented and discussed. The overall performance was obtained by summing up the optimum performances of the top and bottom junctions.

##### Results of the n- $\text{Cu}_2\text{O}$ / p- $\text{Cu}_2\text{O}$ top junction.

The variation of the top n- $\text{Cu}_2\text{O}$ /p- $\text{Cu}_2\text{O}$  base layer junction thickness in the range  $0.001$  to  $10\mu\text{m}$  was obtained under  $1000\text{Wm}^{-2}$  illumination, Figure 3. The results are  $V_{oc} = 1.20\text{V}$ ,  $J_{sc} = 10.67\text{mA/cm}^2$ ,  $\text{FF} = 79.33\%$  and  $\eta = 10.18\%$  obtained at the optimum thickness of  $0.07\mu\text{m}$ .

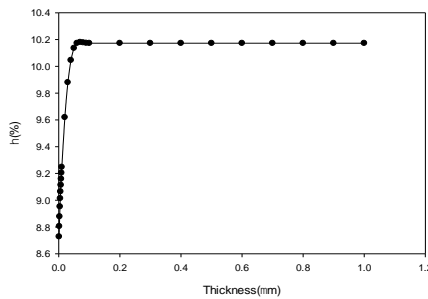


Figure 3: Graph of Efficiency Variation against Thickness for n-  $\text{Cu}_2\text{O}$  / p-  $\text{Cu}_2\text{O}$  Top Junction

The efficiency value of  $10.18\%$  obtained in this work is much higher than the previously reported experimental result of  $4.21\%$  for a homojunction  $\text{Cu}_2\text{O}$  solar cell [24]. The result is also an improvement over a simulation conversion efficiency result of  $5.44\%$  for a single heterojunction  $\text{Cu}_2\text{O}$ -based solar cell [25]. However, highest single junction efficiency value of  $9.54\%$  was reported for  $\text{Cu}_2\text{O}$ -based heterojunction obtained experimentally [26]. All the reported results were obtained under unconcentrated sunlight AM1.5.

##### Results of the single n-GaSb/ p-GaSb bottom junction

The results presented in this section were obtained for the performance of n-GaSb/ p-GaSb base junction under two different illumination conditions. The conditions are the normal  $1000\text{Wm}^{-2}$  and that of the radiation reaching the junction  $622\text{Wm}^{-2}$ , when used in the tandem cell as the base subcell.

Firstly, the results of the n-GaSb/ p-GaSb single junction base layer thickness variation in the range  $0.1$  to  $1 \times 10^4 \mu\text{m}$  using  $1000 \text{Wm}^{-2}$  were obtained. This was done in order to study the effects of the variation of base layer thickness on the performance of the junction under normal illumination condition. The best results of  $V_{oc}=0.38\text{V}$ ,  $J_{sc}=56.30\text{mA/cm}^2$ ,  $\text{FF}=76.11\%$  and  $\eta=16.34\%$  were obtained at the thickness of  $3 \times 10^3 \mu\text{m}$ , Figure 4. This efficiency is the optimum value obtained at the stated thickness.

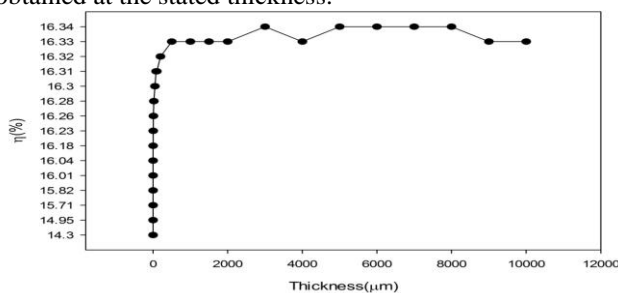


Figure 4: Graph of Efficiency against Thickness for n-GaSb/p-GaSb Single Junction under  $1000\text{Wm}^{-2}$

It is clear from Figure 4 that efficiency is relatively constant above 16.34% but with slight fluctuations. The fluctuations were as a result of the rise and fall in  $J_{sc}$  with increasing thickness, while the  $V_{oc}$  remained unchanged. The fluctuation is attributed to thermalization effect.

Secondly, the results of the study of n-GaSb/ p-GaSb base layer thickness in the range 0.1 to  $1 \times 10^4 \mu\text{m}$  using  $622 \text{Wm}^{-2}$  are presented. This study was to obtain the effects of variations of the base layer thickness on the performance of the junction under the stated radiation when used in the tandem cell as the base subcell. The best results were obtained at the thickness of 6.0  $\mu\text{m}$  these include  $V_{oc} = 0.37\text{V}$ ,  $J_{sc} = 46.14 \text{mA/cm}^2$ ,  $\text{FF} = 77.10\%$  and  $\eta = 21.01\%$ , Figure 5.

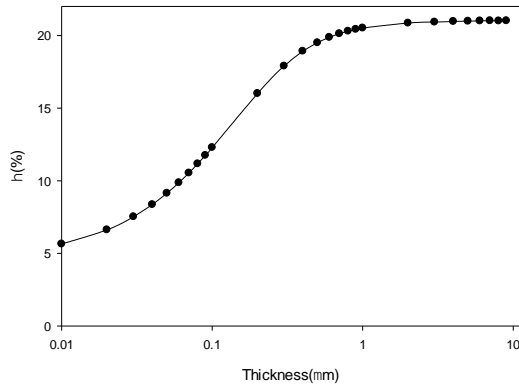


Figure 5. Graph of Efficiency against Thickness for n-GaSb/p-GaSb Bottom Junction under  $622 \text{Wm}^{-2}$

Generally, the effect of base layer thickness variation on the solar cell output parameters showed that, power conversion efficiency increased as a result of increase in photocurrent due to enhanced flux absorption. After the efficiency had reached its maximum value, it thereafter decreased as a result of reduction in  $V_{oc}$  which was due to increase in reverse saturation current ( $J_0$ ). Similarly,  $J_{sc}$  decreased when the cells thickness exceeded certain optimum value due to recombination phenomenon. This was as a result of the free charge carriers generated much deeper into the bulk material had to travel longer distances before being collected. However, the smallest thickness value that showed better conversion efficiency was taken as the optimum thickness.

However, the efficiency of 21.01% obtained for the n-GaSb/p-GaSb bottom subcell under unconcentrated sunlight in this work is approaching the theoretical value of 28% [15] and is higher than the reported value of 15% [27]. This indicates that n-GaSb/p-GaSb is more efficient when used as a bottom material since it has higher efficiency than when used as an independent single junction solar cell in which it has lower efficiency.

Finally, the overall performance of the proposed tandem solar cell was obtained according to equation (13) that is using the efficiencies of both top n-Cu<sub>2</sub>O/p-Cu<sub>2</sub>O and n-GaSb / p-GaSb bottom subcells forming the proposed four-terminal tandem solar cell. The efficiency obtained was 31.2%.

## 5. Conclusion

This work has successfully simulated and determined the performance of two junctions, four terminals tandem solar cell. The tandem solar cell was made up of top n-Cu<sub>2</sub>O/p-Cu<sub>2</sub>O and bottom n-GaSb/p-GaSb Junctions using SCAPS 1D solar cell simulation software. The efficiency of the Cu<sub>2</sub>O/GaSb tandem solar cell indicates a promising future for the individual materials. The efficiency of 10.18% obtained for Cu<sub>2</sub>O under  $1000 \text{Wm}^{-2}$  is an improvement over reported values in literatures, as at the time of writing this paper. The GaSb efficiency of 21.01% under  $622 \text{Wm}^{-2}$  shows remarkable increase compared with the result under  $1000 \text{Wm}^{-2}$  of the same material. This attributed to thermalization effect being greatly reduced when the material was used as a bottom layer of the tandem solar cell. The efficiency of the tandem solar cell of 31.2% clearly surpassed the Shockley-Queisser efficiency limit. This was achieved by the tandem structure, in which the top junction absorbed the high energy photons of the solar flux and reduced the thermalisation effect in the bottom junction.

## REFERENCES

- [1] Rashmi, S. (2012). Solar Cell. International Journal of Scientific and Research Publications, 2(7): 1-5 ISSN 2250-3153.
- [2] Singal, R.K; (2009): Non-Conventional Energy Resources. S.K Kataria & Sons. Page 16.
- [3] Antonio, L. and Steven, H. (2003). *Handbook of Photovoltaic Science and Engineering*. John Wiley and Sons Ltd. Pp 364,368 and 83.
- [4] Wikipedia :[https://en.wikipedia.org/wiki/Solar\\_cell#History-20/10/2020\(1:30pm\)](https://en.wikipedia.org/wiki/Solar_cell#History-20/10/2020(1:30pm))
- [5] Andreani, L.C; Bozzola, A; Kowalczewski, P; Liscidini, M; and Redorici, L; (2019): Silicon Solar Cells ; Towards the Efficiency Limit. Advances in Physics. Vol. 4, No. 1, Page 125-148.

- [6] Green, M.A; Dunlop, E.D; Hohl-Ebinger, J; Yoshita, M; Kopidakis, N; and Hao, X; (2020): Solar Cell Efficiency Tables (Version 56). John Wiley & Sons Ltd. Page 630.
- [7] Kayes, B.M; Nie, H., Twist, R., Spruytte, S. G., Reinhardt, F., Kizilyalli, I.C and Higashi, G.S; (2011): 26% Conversion Efficiency, a New Record for Single Junction Solar Cells Under 1 Sun Illumination. Alta Devices, Inc, Santa Clara USA. Pages 4-8.
- [8] Shockley, M. and Queisser, H. J. (1961). Detailed Balance Limit of Efficiency of *p-n* Junction Solar Cells. Journal of Applied Physics. 32, (1961): 510-519. doi: 10.1063/1.1736034
- [9] King, G.C; (2018): Physics of Energy Sources. John Wiley & Sons Ltd. Page 246.
- [10] Mertens, K; (2014): Photovoltaics Fundamentals, Technology and Practice. John Wiley & Sons Ltd. Page 112.
- [11] Brenton, B. (2002). The Basic Physics and Design of III-V Multijunction Solar Cells. NREL's III-V research group in the summer of 2002.
- [12] Eduardo, F. F., Antonio, J. G. and Greg, P. S. (2015). Multijunction Concentrator Solar Cells: Analysis and Fundamentals. High Concentrator Photovoltaics, Green Energy and Technology, pp:9-37 DOI 10.1007/978-3-319-15039-0\_2.
- [13] Abdu, Y. and Musa, A.O. (2009). Copper (I) Oxide (Cu<sub>2</sub>O) Based Solar Cells - A Review. Bayero Journal of Pure and Applied Sciences, 2(2): 8 – 12.
- [14] Zhu, L. (2012). Development of Metal Oxide Solar Cells through Numerical Modelling. (Doctoral Thesis). Institute for Renewable Energy and Environment Technologies, University of Bolton.
- [15] Bouzid, F. and Dehimi, L. (2012). Performance Evaluation of a GaSb Thermophotovoltaic Converter. Revue des Energies Renouvelables, 15(3): 383 – 397.
- [16] White, T. P., Lal, N. N. and Catchpole, K. R. (2013). Tandem Solar Cells Based on High- Efficiency c-Si Bottom Cells: Top Cell Requirements for >30% Efficiency. Journal of Photovoltaics. DOI: 10.1109/JPHOTOV.2013.2283342.
- [17] Millman, J. and Halkias, c. c. (2005). Integrated Electronics: Analog and Digital Circuit and System. Tata McGraw-Hill Publishing Company New Delhi. pp 34.
- [18] Singh, P. and Ravindra, N.M. (2012). Temperature Dependence of Solar Cell Performance and Analysis. Solar Energy Materials and Solar Cells, 101 (2012): 36–45.
- [19] Filipič, M., Löper, P., Niesen, B., De Wolf, S., Krč, J., Ballif, C. and Topič, M.(2015). CH<sub>3</sub>NH<sub>3</sub>PbI<sub>3</sub> perovskite / silicon tandem solar cells: characterization based optical simulations. Optical Society of America, 23(7): .DOI:10.1364/OE.23.00A263.
- [20] Reynolds, S. and Smirnov, V. (2015). Modelling performance of two- and four-terminal thin-film silicon tandem solar cells under varying spectral conditions. *Science direct*. 84 (2015): 251 – 260. DOI: 10.1016/j.egypro.2015.12.321.
- [21] Musk, E. (2016). Hybrid tandem solar cells. RVO Croeselaan 15, 3521 BJ Utrecht, the Netherlands, in close collaboration with TKI Urban Energy, Arthur van Schendelstraat 550, 3511 MH Utrecht, the Netherlands. Ref. number: IPZ1500051. Pp 26, 31 and 32.
- [22] Kjetil, K. (2019). Characterization of Li doped magnetron sputtered Cu<sub>2</sub>O thin films. (Master Thesis). Department of Chemistry, Faculty of mathematics and natural Sciences, University Of Oslo.
- [23] Dutta, P. S. and Bhat, H. L. (1997).The physics and technology of gallium antimonide: An emerging optoelectronic material. Journal of applied physics, 81(9): 5821- 5870.
- [24] Minami, T; Yamazaki, J; and Miyata, T; (2016): Efficiency Enhanced Solar Cells with a Cu<sub>2</sub>O Homojunction Grown Epitaxially on p-Cu<sub>2</sub>O:Na Sheets by ElectroChemical Deposition. MRS Communications. Vol. 6, No.4, page 416-420.
- [25] Rizi, M.T; Abadi, M.H.S; Ghaneji, M; (2018): Two Dimensional Modelling of Cu<sub>2</sub>O Heterojunction Solar Cells Based on β-Ga<sub>2</sub>O<sub>3</sub> Buffer. Physics Optik. DOI: 10.1016/J.IJLEO.2017.11.028.
- [26] Liu, Y; Zhu, J; Cai, L; Yao, Z;Duan, C; Zhao, Z; Zhao, C; and Mai, W; (2020): Solution Processed High Quality Cu<sub>2</sub>O Thin Films as Hole Transport Layers for Pushing the Conversion Efficiency Limit of Cu<sub>2</sub>O/Si Heterojunction Solar Cells. RRL Solar. DOI: 10.1002/solr.201900339.
- [27] Khvostikov, V.P; Rastegaeva, M.G; Khvostikova, O.A; Sorokina, S.V; Malevskaya, A.V; Shvarts, M.Z; Andreev, A.N; Davydov, D.V and Andreev, V.M; (2006): High Efficiency (49%) and High Power Photovoltaic Cells Based on Gallium Antimonide. Semiconductors. Vol. 40, No. 10, Page 1242-1246.